ISSN 1674-1056
http://cpb.iphy.ac.cn
http://iopscience.iop.org/cpb
中国物理 B
Chinese Physics
中国物理
Chinese Physics B

Anisotropic stimulated emission cross-section measurement in Nd:YVO_4

Rui Guo(郭瑞), Yijie Shen(申艺杰), Yuan Meng(孟鸢), Mali Gong(巩马理)

Citation: Chin. Phys. B . 2019, 28(4): 044204. **doi:** 10.1088/1674-1056/28/4/044204
Journal homepage: http://cpb.iphy.ac.cn; http://iopscience.iop.org/cpb

What follows is a list of articles you may be interested in

Active hyperspectral imaging with a supercontinuum laser source in the dark

Zhongyuan Guo(郭中源), Yu Liu(刘煜), Xin Zheng(郑鑫), Ke Yin(殷科)

Chin. Phys. B . 2019, 28(3): 034206. **doi:** 10.1088/1674-1056/28/3/034206

1.5-MHz repetition rate passively Q-switched Nd: YVO_4 laser based on WS_2 saturable absorber

Xi Wang(王茜), Lu Li(李璐), Jin-Ping Li(李金萍), Yong-Gang Wang(王勇刚)

Chin. Phys. B . 2017, 26(4): 044203. **doi:** 10.1088/1674-1056/26/4/044203

Frequency doubled femtosecond Ti:sapphire laser with an assisted enhancement cavity

Jin-Wei Zhang(张金伟), Hai-Nian Han(韩海年), Lei Hou(侯磊), Long Zhang(张龙),Zi-Jiao Yu(于子蛟), De-Hua Li(李德华), Zhi-Yi Wei(魏志义)

Chin. Phys. B . 2016, 25(1): 014205. **doi:** 10.1088/1674-1056/25/1/014205

Sensitive absorption measurements of hydrogen sulfide at 1.578 μm using wavelength modulation spectroscopy

Xia Hua, Dong Feng-Zhong, Wu Bian, Zhang Zhi-Rong, Pang Tao, Sun Peng-Shuai, Cui Xiao-Juan, Han Luo, Wang Yu

Chin. Phys. B . 2015, 24(3): 034204. **doi:** 10.1088/1674-1056/24/3/034204

Off-resonant double-resonance optical-pumping spectra and their application in a multiphoton cesium magneto-optical trap

Yang Bao-Dong, He Jun, Wang Jun-Min

Chin. Phys. B . 2014, 23(5): 054205. **doi:** 10.1088/1674-1056/23/5/054205

Anisotropic stimulated emission cross-section measurement in Nd:YVO_4

Rui Guo(郭瑞)[1], Yijie Shen(申艺杰)[1], Yuan Meng(孟鸢)[1], and Mali Gong(巩马理)[1,2,†]

[1] *Department of Precision Instrument, State Key Laboratory of Precision Measurement and Instruments, Tsinghua University, Beijing* 100084, *China*
[2] *Department of Precision Instrument, State Key Laboratory of Tribology, Tsinghua University, Beijing* 100084, *China*

(Received 16 August 2018; revised manuscript received 18 January 2019; published online 19 March 2019)

As a crucial parameter in the design and analysis of laser performances, stimulated emission (SE) cross-section is currently considered to be dependent on several factors, such as temperatures and eigen-polarizations for anisotropic crystals. In contrast with these factors, impact of propagating directions upon SE cross-section has garnered less attention. In this paper, to investigate the SE cross-section in arbitrary propagating directions, fluorescence spectra for the transition $^4F_{3/2} \rightarrow {}^4I_{11/2}$ in Nd:YVO_4 are measured in different propagating directions. Based on Fuchtbauer–Ladenburg equation model, the propagating direction-dependent SE cross-section spectra in Nd:YVO_4 are obtained for the first time, to our best knowledge. A novel concept of anisotropic SE cross-section is proposed to interpret the propagating direction-dependent effect. The experiment results reveal that for an arbitrary propagating direction the SE cross-section of *e* light around 1064 nm can be expressed as a superposition from two principle axial propagating directions with a weight of plane projection.

Keywords: solid-state lasers, stimulated emission cross-section, Nd:YVO_4, laser spectroscopy

PACS: 42.55.Ah, 42.60.Lh, 42.62.Fi, 42.60.By **DOI:** 10.1088/1674-1056/28/4/044204

1. Introduction

As a key parameter for laser gain media, the stimulated emission (SE) cross-section plays a crucial role in modeling output performances of various laser systems.[1,2] SE cross-section spectra of different transitions have been measured in many previous reports, such as $^4F_{3/2} \rightarrow {}^4I_{11/2}$ for Nd^{3+} ions-doped materials,[3] $^2F_{5/2} \rightarrow {}^2F_{7/2}$ for Yb^{3+} ions-doped materials,[4] and $^3F_4 \rightarrow {}^3H_6$ for Tm^{3+}-doped materials.[5] The SE cross-section at a certain emission wavelength is affected by a set of factors. For example, several groups investigated the temperature dependence of SE cross-section on crystals.[3,6,7] For Yb-doped materials, the SE cross-section is dependent on doping concentration in highly doped cases.[8] SE cross-section also has strong relation with polarizations for anisotropic crystals, such as π polarization and σ polarization in uniaxial crystals[9–11] and *x* polarization, *y* polarization, *z* polarization for biaxial crystals.[12] However, SE cross-section was only considered for cases with propagating directions parallel to principle axes in these previous investigations. It remains vague to date that how the SE cross-section is affected by propagating directions. The dependence upon the propagating direction of SE cross-section is of great significances in applications such as the innoslab laser systems[13–15] and zigzag slab laser systems.[16] A multi-folded light path structure was adopted in these laser systems to increase gain length, while the propagating direction deviates from principle axes during light propagation. This has motivated us to reveal the dependence between propagating direction and SE cross-section, and it is helpful for designing and analyzing multi-folded light path laser systems.

Nd:YVO_4 is an excellent high gain crystal which has been widely applied in high-power lasers.[17–20] As a typical uniaxial crystal, Nd:YVO_4 shares the same polarization-dependent characteristic with other uniaxial crystals like Nd:YLF and Nd:$GdVO_4$, so it is adopted in our experiment to investigate the propagating direction-dependent effect of SE cross-section. In this paper, the Fuchtbauer–Ladenburg equation is used as the methodology to calculate the SE cross-section of different propagating directions in Nd:YVO_4. Using the Fuchtbauer–Ladenburg equation, the SE cross-section can be obtained by measuring the fluorescence spectra. Here, fluorescence spectra for transitions around 1 μm in Nd:YVO_4 are stimulated by a laser diode pumped system. The propagating direction-dependent SE cross-section spectra in Nd:YVO_4 are measured for the first time, to the best of our knowledge. The relationship between peak SE cross-section around 1064.4 nm and propagating direction is also investigated.

2. Principle for anisotropic SE cross-section measurement

2.1. SE cross-section of eigen polarizations in uniaxial crystals

The anisotropic crystals with polarized-dependent emission characteristics have different SE cross-section spectra for

†Corresponding author. E-mail: gongml@mail.tsinghua.edu.cn

© 2019 Chinese Physical Society and IOP Publishing Ltd

different eigen polarizations. Uniaxial crystals have one c axis (optical axis) and two perpendicular a axes in Cartesian coordinates. The refractive ellipsoid in a uniaxial crystal is schematically depicted in Fig. 1, where the z axis represents the c axis, the x, y axes respectively stand for two a axes, and $\boldsymbol{o}$ and $\boldsymbol{e}$ are the unit vectors of the polarization of the o light and the e light respectively. For a linear polarized light wave propagating along the a axis, as shown in Fig. 1(a), the SE cross-section of the e light and the o light refers to σ_c and σ_a, respectively. Since the SE cross-section of two eigen polarizations has been clearly investigated,[10,11] the SE capability of an arbitrary polarization in yOz can be characterized by dividing it into two eigen polarizations. For a linear polarized light wave propagating along the c axis, as shown in Fig. 1(b), the SE cross-section is σ_a for an arbitrary polarization due to the symmetry about c axis. In a word, the SE capability of an arbitrary polarization for axial propagating directions can be decided by SE cross-section of eigen polarizations.

2.2. Propagating direction-dependent SE cross-section in uniaxial crystals

Although the SE cross-section of eigen polarizations can be used to describe SE capability of an arbitrary polarization for axial propagating directions, the SE cross-section for non-axial propagating directions is hard to be understood by only considering eigen polarizations. For instance in Fig. 1(c), when the wave vector $\boldsymbol{k}$ in xOz plane deviates from the z axis by an angle θ, $\boldsymbol{o}$ is still parallel to the y axis. However, $\boldsymbol{e}$ will deviate from x axis with θ. It can be deduced that the SE cross-section of $\boldsymbol{e}$ is dependent on θ due to the different value at $\theta = 0$ and 90°. Hence, a direction-dependent property of SE cross-section is necessary to be introduced. The SE cross-sections of polarizations $\boldsymbol{o}$ and $\boldsymbol{e}$ under different θ are to be investigated.

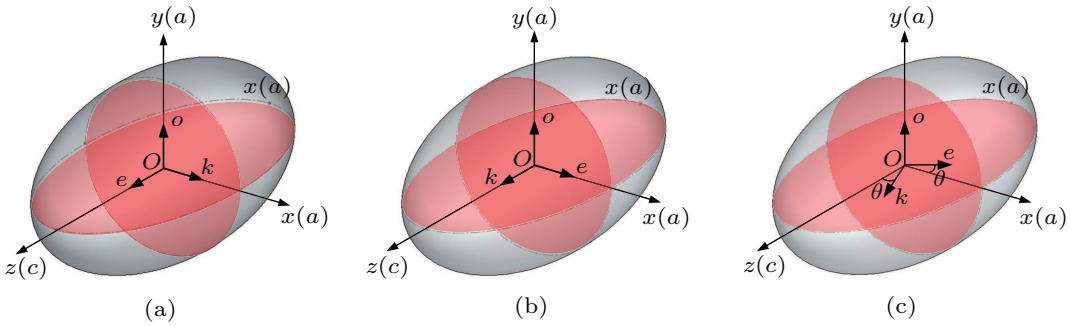


Fig. 1. Eigen polarization directions in uniaxial crystals. (a) $\boldsymbol{k}$ along the x axis; (b) $\boldsymbol{k}$ along the z axis; (c) $\boldsymbol{k}$ deviated from principle axis.

2.3. Methods for SE cross-section measurement

The SE cross-section spectrum can be measured by two methods: laser operation method and Fuchtbauer–Ladenburg equation method. Laser operation method uses the laser performances such as slope efficiency, and threshold power to measure the gain. Thus, SE cross-section can be calculated via combining the overlap efficiency between mode beams and pump beams.[7,21] In these studies, the overlap efficiency is invariant because the propagating directions of laser is axial. However, the overlap efficiency is dependent on propagating directions in our study. The accurate knowledge of overlap efficiency of different propagating directions is hard to be solved, which makes it difficult to decouple SE cross-section from gain of the laser. Therefore, the Fuchtbauer–Ladenburg equation method is adopted in this paper.

The Fuchtbauer–Ladenburg equation is shown as below:

$$\sigma_{\mathrm{em}}(\lambda) = \frac{(\bar{\lambda})^4}{8\pi c n^2 \tau_{\mathrm{rad}}} \cdot \frac{I(\lambda)}{\int I(\lambda)\,\mathrm{d}\lambda}, \tag{1}$$

where λ refers to the wavelength of the fluorescent emission. n refers to the refractive index. τ_{rad} is the fluorescence lifetime. $I(\lambda)$ is the intensity of the fluorescent emission at λ. The SE cross-section spectrum is proportional to the normalized fluorescent emission spectrum. Hence, the SE cross-section spectrum for a certain propagating direction can be obtained by measuring the corresponding spectrum of the fluorescent emission.

3. Experimental setup

The experimental setup to measure the fluorescent emissions is illustrated in Fig. 2. A laser diode (LD) from nLIGHT Photonics emitting at 808 nm is used as pump source to stimulate fluorescent emissions. The parameter of output coupling fiber is 400/0.22. Using two coupled lenses, the pump light with 10-W output power is focused into the crystal. A maximum pump-induced temperature increase of 10 °C is observed via a thermal camera. Three 12 mm×12 mm×2 mm Nd:YVO_4 specimens (0.3 at.%) are processed into a special shape. The c axis of the Nd:YVO_4 crystals is parallel to one of the 12-mm direction, marked as a dash line in Fig. 2. Since the critical angle of total internal reflection in Nd:YVO_4 is only about 30°, the crystals are cut into the wedge shape in order to make fluorescent emissions with large angles refract out the

Nd:YVO_4. As presented in Fig. 3 (a), the angle between the end face 2 and the wedge face 1, and the angle between the side face 2 and the wedge face 2 are both 30°. The side face 1 is grinded in order to prevent parasitic oscillators inside the crystals. The Nd:YVO_4 crystals are mounted on copper heat sinks, which are cooled by circulating water. A polarizer is applied to discriminate the *o* light and the *e* light. A single mode fiber (SMF) is placed after the polarizer, and then connect to an optical spectrum analyzer (Agilent 86142B). By adjusting the directions of polarizer and SMF aligned to the corresponding fluorescence refracted from the crystal, the fluorescent emission spectra of different propagating directions in the Nd:YVO_4 crystals are measured for *o* light and *e* light. Since the NA of SMF is about 0.13 (≈ 8°), an aperture is inserted between the measured crystal and the polarizer as a field stop (Fig. 3(b)), which restricts the acceptance angle to less than 5°. Considering $n \approx 2$ for Nd:YVO_4, the fluorescence with an angular resolution of 2.5° inside the crystals is received by SMF.

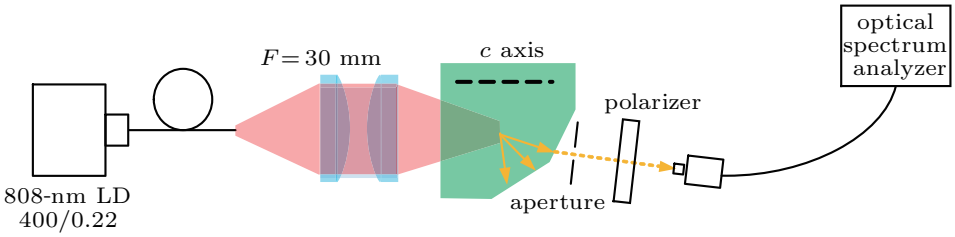


Fig. 2. Experiment Setup of fluorescent emissions measurement system.

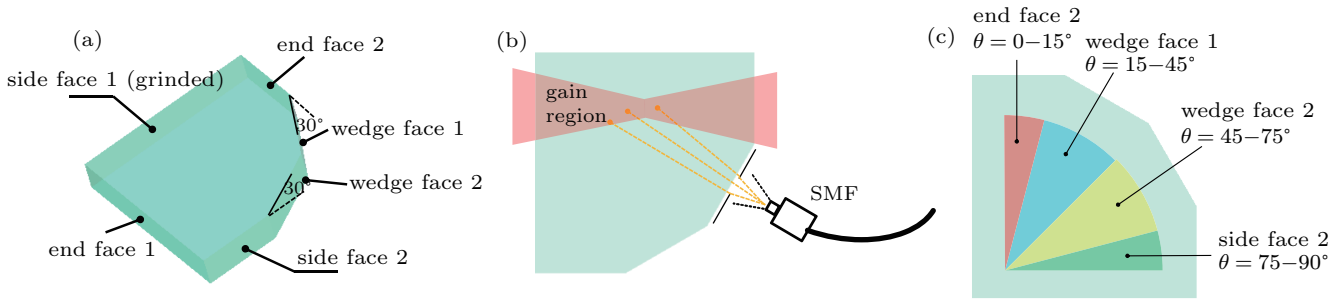


Fig. 3. (a) diagram of the wedged Nd:YVO_4 crystals (The large faces of the crystals are unpolished. The end faces 1, 2, the wedge faces 1, 2, and the side face 2 are polished); (b) Diagram of the fluorescent signal received by SMF (polarizer is omitted to be convenient); (c) the exiting surfaces corresponding to fluorescent emissions of different propagating directions.

4. Data analyses and discussions

The fluorescent emission spectra are acquired at different θ values ($0° \leq \theta \leq 90°$) for three Nd:YVO_4 specimens respectively, where $\theta = 0°$ and $\theta = 90°$ correspond to the cases of wave vector $\boldsymbol{k}$ parallel and perpendicular to the *c* axis (as shown in Fig. 1(b) and Fig. 1(a), respectively). The fluorescent emissions of different directions are received after four different surfaces, as shown in Fig. 3(c). The fluorescent emissions with $\theta = 0°$–$15°$, $\theta = 15°$–$45°$, $\theta = 45°$–$75°$, and $\theta = 75°$–$90°$ are measured by the optical spectrum analyzer after the end face 2, the wedge face 1, the wedge face 2 and side face 2, respectively. The spectra for both the *e* light and the *o* light are acquired for wavelength range between 1050 nm–1110 nm for transition $4F_{3/2} \rightarrow 4I_{11/2}$ with a resolution of 0.06 nm. The power of emission peak is about several tens of pW to several hundreds of pW. Combined with other parameters in Eq. (1), the SE cross-section spectra of the *o* light and the *e* light are calculated: the fluorescence lifetime τ_{rad} is 98 μs;[9] the refractive index *n* is considered as variable for different θ, according to refractive ellipsoid equation.

4.1. SE cross-section spectra of the *e* light

Figures 4(a)–4(j) illustrate the SE cross-section spectra of the *e* light of three Nd:YVO_4 specimens at $\theta = 0°$, $10°$, …, $90°$ accordingly. The spectra of $\theta = 0°$ and $\theta = 90°$ correspond to the σ-polarization and the π-polarization, respectively, which are consistent with results in Ref. [10]. It can be observed that emission peaks of the σ-polarization locate around 1062 nm, 1064 nm, 1066 nm, 1072 nm, 1084 nm, and 1087 nm. Meanwhile, the positions of the emission peaks of π polarization (in Fig. 4(j)) are around 1064 nm, 1073 nm, and 1085 nm, and the intensity of the emission around 1064 nm is much stronger than the others.

When θ increases from 0°, the emission peaks around 1062 nm and 1066 nm start to decrease, while the intensity of the emission peak around 1064 nm grows gradually. The positions of the peaks around 1072 nm and 1084 nm also gradually transfer to 1073 nm and 1085 nm. For the intermediate state such as $\theta = 40°$, $50°$, the spectra around 1084 nm be-

come more flat owing to the superposition of emission spectra around 1084 nm and 1085 nm. Thus, the shapes of the spectra of SE cross-section for the e light gradually approach to that in Fig. 4(j). The relationship is coincident for all three Nd:YVO_4 specimens. These results reveals that the spectra of SE cross-section for the transition $^4F_{3/2} \rightarrow {}^4I_{11/2}$ are direction-dependent in Nd:YVO_4. The SE cross-sections at 1064.4 nm vary from 5.5×10^{-19} cm^2, 6.5×10^{-19} cm^2, and 5.9×10^{-19} cm^2 to 13.4×10^{-19} cm^2, 14.2×10^{-19} cm^2, and 16.0×10^{-19} cm^2 when θ increases from 0° to 90°, for three specimens respectively, which are close to the values reported by Cornacchia[10] and Peterson.[11]

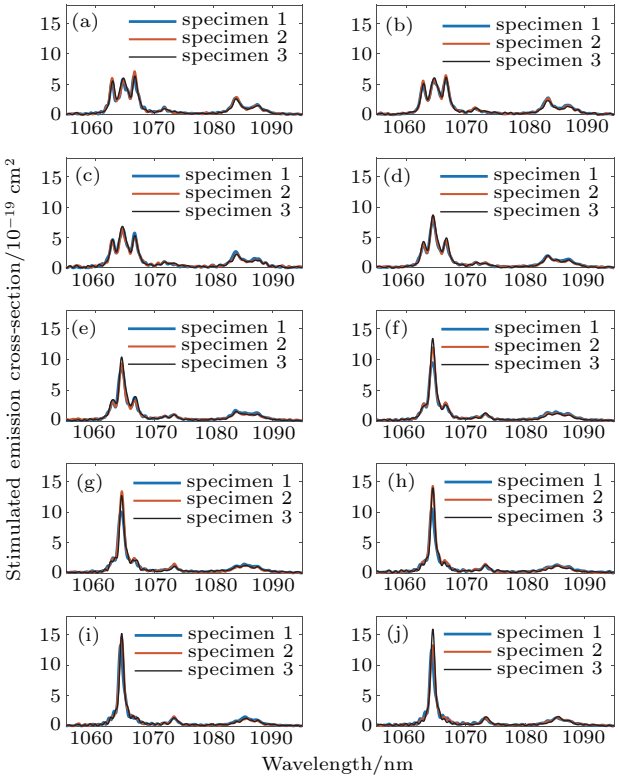


Fig. 4. SE cross-section spectra of the e light at $\theta = 0°, 10°, \ldots, 90°$ (0°–90° corresponding to panels (a)–(j)).

4.2. SE cross-section spectra of the *o* light

The SE cross-section spectra of the o light of three specimens at $\theta = 0°$–$10°, \ldots, 90°$ are given in Figs. 5(a)–5(j). It can be discovered that the intensity of emission around 1064 nm is generally close to that around 1062 nm and 1066 nm. Although the SE cross-section spectra of the o light should be consistent in any directions ideally, the measured spectra in our experiment fluctuate by to some extent. At several angles (such as $\theta = 60°$ in specimen 1), the intensity of emission around 1064 nm can exceed that of 1062 nm and 1066 nm. The minimum and maximum SE cross-section values measured from all angles of three specimens are 5.5×10^{-19} cm^2 and 7.9×10^{-19} cm^2. Since the higher SE cross-section at 1064.4 nm of the o light is also observed in previous reports in different specimens,[10,11,22] we think the measured SE cross-section spectra and the SE cross-section value at 1064.4 nm of the o light fluctuate in a reasonable range.

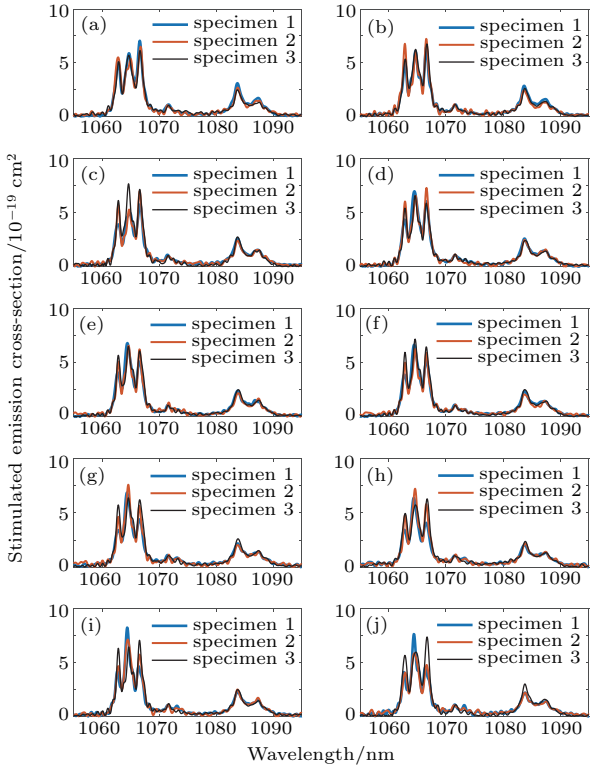


Fig. 5. SE cross-section spectra of the o light at $\theta = 0°, 10°, \ldots, 90°$ (0°–90° corresponding to panels (a)–(j)).

4.3. Anisotropic SE cross-section at 1064 nm

The characteristics of direction-dependent SE cross-section spectra in Nd:YVO_4 result in the anisotropic SE cross-section at a certain emission wavelength. Since the emission peak around 1064 nm is the most common wavelength in Nd:YVO_4 lasers, here we discuss the anisotropic SE cross-section at the wavelength of 1064.4 nm. The peak SE cross-section around 1064 nm under different propagating directions is given in Figs. 6(a) and 6(b) for e light and o light, respectively.

In Fig. 6(a), the SE cross-section grows slowly in $\theta = 0°$–20°, and then rise rapidly in $\theta = 20°$–70° , and finally the increase is saturated in $\theta = 70°$–90°. Due to the symmetry, it can be expected that the relationship of the SE cross-section against θ will be symmetrical to $\theta = 90°$ when $\theta = 90°$–180°. We assume that SE cross-section for an arbitrary propagating direction can be expressed as a superposition from two principle axial propagating directions with θ-dependent weights. Considering the physical origin that SE cross-section is proportional to normalized intensity of the fluorescence spectrum (Eq. (1)), the weight factor should be the square of cosine and sine function.

$$\sigma_e(\theta) = \sigma_{em,\sigma}\cos^2\theta + \sigma_{em,\pi}\sin^2\theta. \quad (2)$$

The measured SE cross-section of different θ in Fig. 6(a) is fitted into the functional form of Eq. (2). The fitted $\sigma_{em,\sigma}$ for three specimens are 5.7×10^{-19} cm^2, 6.7×10^{-19} cm^2, and 6.1×10^{-19} cm^2, and the fitted $\sigma_{em,\pi}$ for three specimens are

12.9×10^{-19} cm^2, 14.4×10^{-19} cm^2, and 16.0×10^{-19} cm^2 respectively. Though the fitted parameters of three specimens have some deviations, the curve plotted in Fig. 6(a) fits the measured points well, which proves the θ-dependent relationship of anisotropic SE cross-section mentioned above. It is verified that the peak SE cross-section (around 1064 nm) of *e* light at a certain propagating direction can be treated as a sum of plane projections of two of the SE cross-section of principle axial propagating directions.

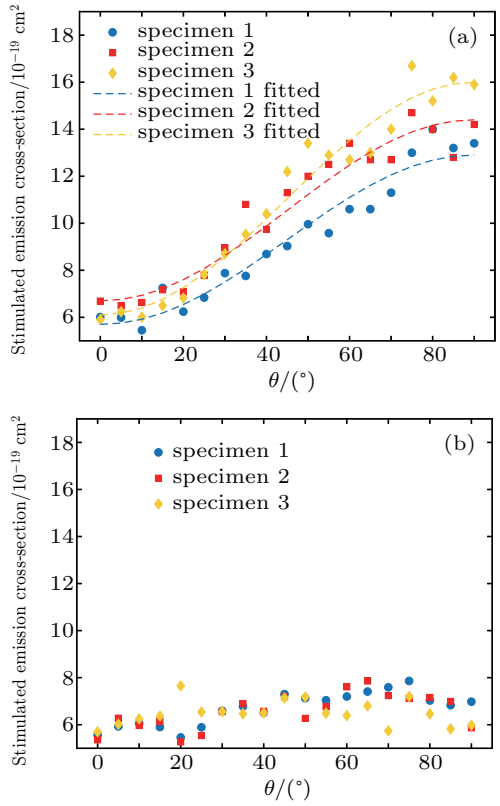


Fig. 6. the peak values of SE cross-section around 1064 nm *versus* different propagating directions (each θ with three measurements) (a) *e* light and (b) *o* light

Equation (2) provides a relationship of the anisotropic SE cross-section in Nd:YVO_4, and characterizes the peak SE cross-section variation of the *e* light around 1064 nm caused by changing of propagating direction. It can not only describe the conventional eigen-porlarized SE cross-section but also characterize a complete propagating direction-dependent effect. Since the gain is proportional to SE cross-section, the laser with different propagating directions will get different gains. Therefore, the relationship is meaningful in the design of multi-folded light path laser systems.

The SE cross-section values of the *o* light in different directions have a fluctuation between 5.5×10^{-19} cm^2 and 7.9×10^{-19} cm^2. The theoretical value should be a constant, however the fluctuations of SE cross-section might be caused by the nonuniformity of the crystal property induced by doped concentration and manufacturing process. The noise of the optical spectrum analyzer might also lead to the fluctuations of the measured SE cross-section values.

5. Conclusions

A new concept of the anisotropic SE cross-section is proposed and verified on Nd:YVO_4 crystals in this paper. With a special wedge-shaped Nd:YVO_4 crystal, the fluorescent emissions from different propagating directions are measured for both *o* light and *e* light. The SE cross-section for $^4F_{3/2} \rightarrow {}^4I_{11/2}$ transitions in Nd:YVO_4 is experimentally found to be propagating direction-dependent for the first time, to our best knowledge. An experimental relationship between the SE cross-section of *e* light and the propagating directions around 1064 nm is found: a superposition of the projection of SE cross-section of *c*-axis and *a*-axis propagations is capable of calculating the SE cross-section for a certain propagating direction. The relationship provides a quantitative reference for laser gain analyses and designs for oscillators and amplifiers with arbitrary laser propagating directions inside the Nd:YVO_4. The proof of anisotropic SE cross-section in Nd:YVO_4 inspires us to explore the properties in other crystals. Other than Nd:YVO_4, anisotropic crystals like $GdVO_4$, YLF, and KGW with various doping ions are anticipated to have the anisotropic SE cross-section property, which is worth studying in future works.

References

[1] Délen X, Balembois F and Georges P 2012 *J. Opt. Soc. USA B* **29** 2339
[2] Nie M, Liu Q, Ji E, Cao X, Fu X and Gong M 2016 *IEEE J. Quantum Electron.* **52** 1
[3] Taira T and Sato Y 2012 *Opt. Mater. Express* **2** 1076
[4] Deloach L D, Payne S A, Chase L L and Smith L K 1993 *IEEE J. Quantum Electron.* **29** 1179
[5] Ramachandran S, Seshadri M, Ferencz Junior J A P, Ratnakaram Y C and Barbosa L C 2014 *Fiber Lasers XI: Technology, Systems, and Applications*
[6] Dong J, Bass M, Mao Y, Deng P and Gan F 2003 *J. Opt. Soc. Am. B* **20** 1975
[7] Krishnan G, Bidin N, Ahmad M F S and Abdullah M 2015 *Laser Phys. Lett.* 12
[8] Patel F D, Honea E C, Speth J and Payne S A 2001 *IEEE J. Quantum Electron.* **37** 135
[9] Balembois F, Georges P and Délen X 2011 *J. Opt. Soc. USA B* **28** 972
[10] Cornacchia F, Turri G, Jenssen H P, Tonelli M and Bass M 2009 *J. Opt. Soc. USA B* **26** 2084
[11] Peterson R, Jenssen H P and Cassanho A 2002 *J. Opt. Soc. USA B* **24** 681
[12] Yoon S, Beecher S and Mackenzie J *The European Conference on Lasers and Electro-Optics* p. CE_P_34
[13] Mao Y, Zhang H, Hao X, Yuan J, Xing J, Xin J and Jiang Y 2016 *Opt. Express* **24** 11017
[14] Heese C, Oehler A E, Gallmann L and Keller U 2011 *Appl. Phys. B* **103** 5
[15] Ma Z, Li D, Hu P, Shell A, Shi P, Haas C R, Wu N and Du K 2007 *Opt. Lett.* **32** 1262
[16] Manni J G 2005 *Opt. Commun.* **252** 117
[17] Liu Q, Nie M, Lu F and Gong M 2016 *IEEE Photon. J.* **8** 1
[18] Chang F L, Sung C L, Huang T L, Wu T W, Cho H H, Liang H C and Chen Y F 2017 *Laser Phys. Lett.* **14** 085803
[19] Liang H C, Wu T W, Tung J C, Tsou C H, Huang K F and Chen Y F 2013 *Laser Phys. Lett.* **10** 105804
[20] Li X, Yu X, Gao J, Peng J, Chen F, Yu J and Chen D 2008 *Laser Phys. Lett.* **5** 429
[21] Mukhopadhyay P K, George J, Sharma S K, Ranganathan K and Nathan T P S 2002 *Opt. Laser Technol.* **34** 357
[22] Sato Y and Taira T 2002 *Jpn. J. Appl. Phys.* **41** 5999